



ISSN: 2230-9926

Available online at <http://www.journalijdr.com>

IJDR

International Journal of Development Research

Vol. 12, Issue, 12, pp. 61077-61082, December, 2022

<https://doi.org/10.37118/ijdr.25974.12.2022>



RESEARCH ARTICLE

OPEN ACCESS

MAPPING-TRIANGULATION INTERPOLATION OF SPARCE GRIDS: THE MaTISG ALGORITHM

*Annibal Hetem Junior

Center for Engineering and Applied Social Sciences/Federal University of ABC

ARTICLE INFO

Article History:

Received 11th October, 2022

Received in revised form

26th October, 2022

Accepted 04th November, 2022

Published online 30th December, 2022

Key Words:

Sparse Grids, Interpolation, Delaunay Triangulation.

*Corresponding author:

Ana Mikaelly Vieira Grangeiro

ABSTRACT

We present the final result of an applied geometry research as an algorithm for interpolation of in N -dimensional sparse grids. The method is based on divide and conquer approach and a "golden rule" chosen for optimization of the problem in specific and general terms, showing good results in a much shorter time. The main steps are Mapping-Triangulation-Interpolation, and we present the results from its application to the problem of estimating age and mass of stellar clusters.

Copyright©2022, Annibal Hetem Junior. This is an open access article distributed under the Creative Commons Attribution License, which permits unrestricted use, distribution, and reproduction in any medium, provided the original work is properly cited.

Citation: Annibal Hetem Junior. 2022. "Mapping-Triangulation Interpolation of Sparce Grids: the Ma TISG algorithm", *International Journal of Development Research*, 12, (12), 61077-61082.

INTRODUCTION

Several problems in applied mathematics involve the use of tables and non-continuous data. In the measurements and information taking environment, the final data set rarely represents a continuous function, although it is usually represented in n -dimensional space. However, despite these characteristics that difficult the use of calculus tools, interpolation of points in these sparse, non-continuous and n -dimensional sets it is one of the needs of many applications. This work was motivated by the need that comes from estimating the ages of stars belonging to open clusters. The process of determining the ages and masses of stars necessarily goes through an interpolation step in the HR diagram (or colour-magnitude diagram – CMD). This important tool of astrophysics was first proposed by astronomers E. Hertzsprung and H. N. Russel in 1908 (Hertzsprung 1908). The HR diagram graphically presents the luminosity versus the effective temperature of the stars in a star cluster. Stars of different ages and masses occupy different positions due to stellar evolution theories. With observational data on the magnitudes of a given star at certain wavelengths, we can compare it to numerical and evolutionary results, which leads us to a good estimate of ages and masses. In this work, we use the theoretical data provided by PARSEC¹, whose tracks (Bressan et al. 2012) are computed for a scaled-solar composition and following specific metallicity relations. They also provide evolutionary tracks.

Traditionally, for a single star, it is enough to plot its data along the curves provided by PARSEC and proceed with an interpolation process, which was often done visually. However, current stellar databases present information with a high degree of accuracy for an immense number of stars. An actual example is the GAIA mission², a European space initiative providing astrometry, photometry, and spectroscopy of more than 1000 million stars in the Milky Way (Gaia 2017). The Gaia Archive contains deduced positions, parallaxes, proper motions, radial velocities, and brightnesses. An example of application is provided by Hetem & Gregorio-Hetem (2019), who used this methodology to estimate the ages of stars in 50 clusters. Figure 1 presents a representation of PARSEC isochrones and some stars belonging to cluster Collinder 205. This huge availability of data leads current astrophysics projects to deal with tens of thousands of stars. Thus, it is necessary to use more precise and automated tools that allow us to speedup the process of estimating ages and masses.

¹ Version v1.2S + COLIBRI PR16 of PARSEC models available on <http://stev.oapd.inaf.it/cgi-bin/cmd>

² <https://gea.esac.esa.int/archive/>

The purpose of this work is to present the idea behind the *MatISG* algorithm, which combines statistics, algebra and geometry in a tool that allows us to make estimates via interpolations in sparse grids with speed and precision.

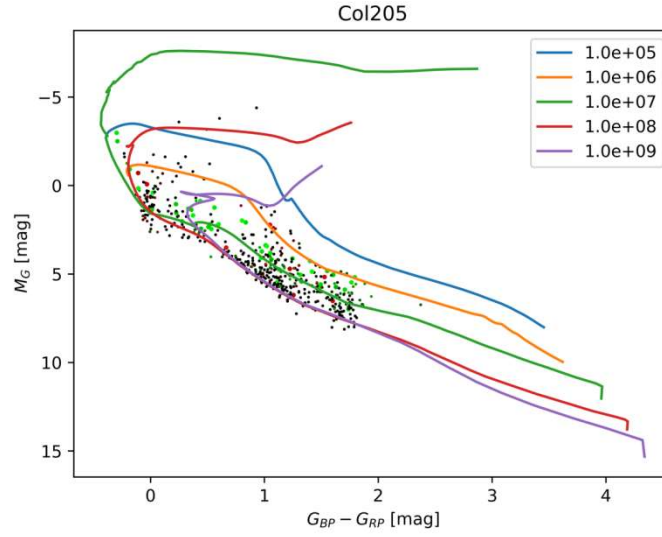


Figure 1. PARSEC isochrones and some stars belonging to cluster Collinder 205. The legend provides the age scale in years.

MATERIALS AND METHODS

This study assumes that we have a sparse set of points $p^M = p(x, y, z \dots, A, B, C \dots)$ in N -dimensional space Ω . The properties of these points allow us to represent them in two different spaces, namely Λ and Γ :

$$\left. \begin{aligned} \lambda^M &= p(x, y, z \dots) \subset \Lambda \\ \gamma^M &= p(A, B, C \dots) \subset \Gamma \end{aligned} \right\} \Lambda \cup \Gamma = \Omega \quad (1)$$

where M is the number of points in N -dimensional spaces, and each has the properties set $(A, B, C \dots) \subset \Gamma$. The dimensions N_Λ and N_Γ are not necessarily equal but are positive integers > 0 and $N_\Lambda + N_\Gamma = N$. The vector $\theta_i = [x_i, y_i, z_i \dots] \in \lambda^M$ represents the position of point i . The two subsets establish a relationship between the two spaces Λ and Γ , and can be treated as a function $\Lambda \rightarrow \Gamma$. Suppose now that we want to obtain approximations of the properties (A, B, C, \dots) for a point $P \in \Omega$ but $P \notin p^M$, which can be interpreted as an external point or observation point. We want to establish a Jacobian transformation matrix to perform the translation from $(x_p, y_p, z_p \dots)$ to $(A_p, B_p, C_p \dots)$, or $\Lambda_p \rightarrow \Gamma_p$ (Weisstein 2018). However, as, in principle, the transformations $\Lambda \rightarrow \Gamma$ are not formally known, nothing can be said about its characteristics, and we are forced to use interpolation techniques.

The obvious (but not the most computationally efficient) way is to calculate the distances between p^M and P in Λ and look for the N_Λ points closest to P , or find the set

$$T^P = \{[\lambda_1, \lambda_2, \lambda_3 \dots, \lambda_{N_\Lambda}] | \delta(\lambda_i, P) < \delta(\lambda_{N_\Lambda+1}, P)\} \quad (2)$$

where $\delta(\lambda_i, P)$ denotes the distance of element i of p^M to P . The T^P points represent the vertices of a polyhedron that contains (or is the closest to) P and from which the properties (A, B, C, \dots) can be interpolated. If the set p^M is relatively large, due to the distances evaluation this step is computationally expensive. For the case where the calculation must be repeated for many external points P , it becomes more and more expensive. This fact led us to look for "divide and conquer" alternatives. And it is at this point that the motivation of this work is outlined. "Divide and conquer" can be implemented in a myriad of ways, all of which will already have a time benefit. We, however, searched for the methodology that was the most effective in terms of both geometry/statistics applied to the problem we want to solve. We call this choice the "golden rule".

The algorithm that we propose follows the following steps (Figure 2):

1. Previously, we divided the Λ space into a given number of continuous contiguous regions R with no points in common, except for their borders. The choice of criteria for this segmentation must strictly follow the golden rule. This is the mapping step.
2. Each region R is subdivided into a set of minimal polyhedra T (like triangles in 2D or tetrahedron in 3D), with no points in common, except for their borders. This is the triangulation step.

2. For each external point P , we look for the region R^P that contains it,

$$\exists R^P | P \underline{\in} R^P \quad (3)$$

where the operator " $\underline{\in}$ " means "geometrically contained", used here so that we are not confused with the " \in " operator applied to sets. If P is not contained in any region R , it is considered not interpolated.

3. Next, we find the minimal polyhedron T^P in R^P that contains P , or

$$\exists T^P \subset R^P | P \in T^P \quad (4)$$

4. We interpolate the properties $\gamma = (A, B, C \dots)$ with the vertices of the polyhedron $[\lambda_1, \lambda_2, \lambda_3 \dots, \lambda_{N_\Lambda}]$, performing

$$\gamma = f(\lambda_1, \lambda_2, \lambda_3 \dots, \lambda_{N_\Lambda}) \quad (5)$$

where $f: \Lambda \rightarrow \Gamma$ is an interpolation function. This is the interpolation step. The interesting work of Goodin, McRae & Seinfeld (1979) presents a good discussion on this field. The main point of performance gain is in the fact that checking if a point is contained within a previously stipulated polyhedron is much faster than calculating all the distances between the points. Another important advantage of this method is that those points that are outside the interpolation area are immediately recognized in step 1, which, in the case of distance checking, can only be identified after trying all possibilities.

Application in the interpolation of ages and masses of stars

Estimating the masses and ages of stars is an important task in astrophysics research, especially for those who study star clusters. Considering the stars belonging to a cluster, their ages and masses are estimated by comparing with the intrinsic colour points, provided by theoretical models (Hetem & Gregorio-Hetem 2007). In this work, we used the theoretical data provided by PARSEC, whose data include color, magnitude, age, and mass obtained by numerical models. With these data, one can generate the colour-magnitude diagram (CMD), or H-R Diagram, whose curves and regions define classes of stars and other astrophysical objects. The PARSEC data are obtained in subsets of pre-established ages a_i in their query and are composed of a series of points not uniformly spaced regarding the other properties. Therefore, each PARSEC point can be represented as

$$p^M = \{\lambda(c, m), \gamma(\alpha, \mu)\} \quad (6)$$

where c represents colour, m , magnitude, α , age and μ , mass (Figure 3).

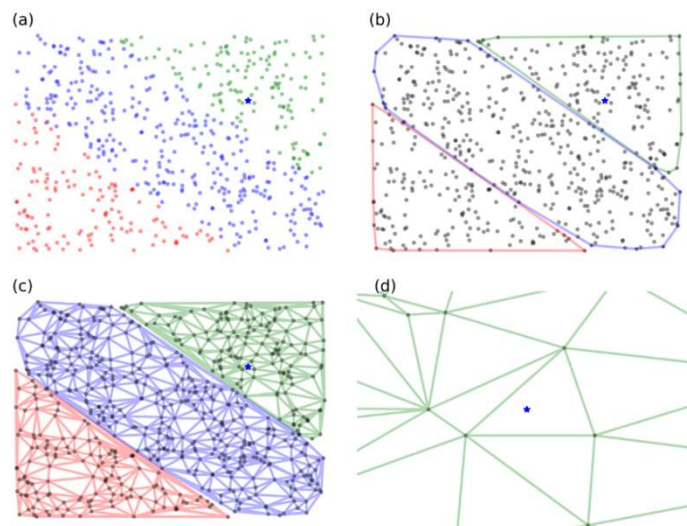


Figure 2. Explanation of the application of the *MaTISG* algorithm. (a) A sparse set of points is divided into regions according to some property or rule, the “golden rule”. The outer point that we want to fit is represented by a blue star. (b) Mapping step: each region determines a polygon that can share points with another region only on its edge. (c) Triangulation step: each polygon is subdivided with triangulation method. (d) This is the interpolation step: window of the subarea with the triangle containing the external point.

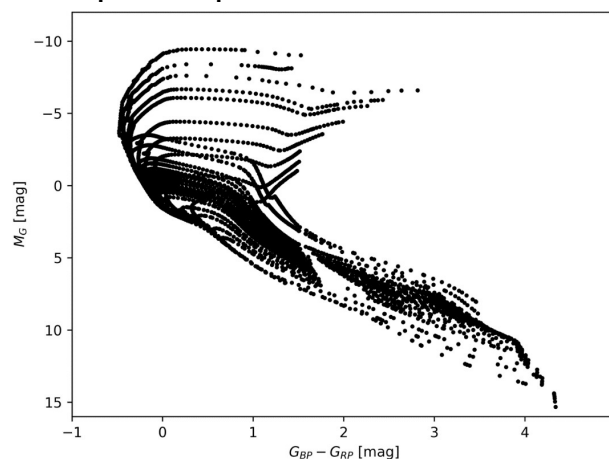


Figure 3. PARSEC original data. Color-magnitude diagram or HR diagram, or $\Lambda=(c, m)$ space. The abscissa axis represents the color, c , obtained from the magnitudes of the GAIA G_{BP} and G_{RP} observations. The coordinate axis represents the GAIA M_G magnitude, m . Each point belongs to an isochronous curve (same age) and represents a mass on this curve, that is, the $\Gamma = (\alpha, \mu)$ space. The units are absolute magnitudes

Step 1 of the algorithm is performed by defining the regions R as the space between the curves containing two consecutive ages as regions. Thus, the golden rule in this case establishes that the polyhedral regions were defined by two PARSEC curves, one with one age and the other with the following age, and two straight line segments that join these curves at their ends. Therefore, the vertices that define each region are given by

$$R_j = \{\lambda_i | \lambda_i \in \alpha_j \vee \lambda_i \in \alpha_{j+1}\} \quad (7)$$

For a set of m ages, $m - 1$ regions are obtained, and (Figure 4)

$$R_1 \cup R_2 \cdots \cup R_{m-1} = \lambda^M \quad (8)$$

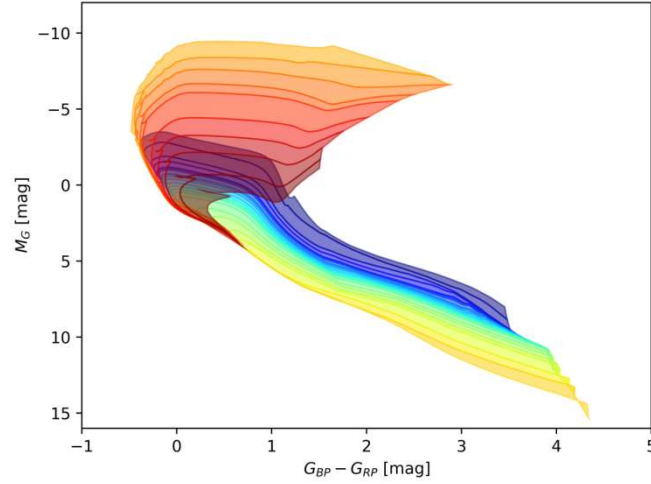


Figure 4. Pairs of isochrones are used to create polygons in the HR diagram. The superposition we see around (0,0) is real and is the result of seeing a 2D projection of a 4D space (see text)

Step 2 of the algorithm consists of performing a Delaunay triangulation (Delaunay 1934) in each region. The result of this step is a set of Q triangles T whose vertices are associated to the age subsets α_j and α_{j+1} of the region R_j . Formally

$$T_k = \{[\lambda_1, \lambda_2, \lambda_3] | \lambda_i \in R_j\} \quad (9)$$

Again, is valid

$$T_1 \cup T_2 \cdots \cup T_Q = R_j. \quad (10)$$

For each star in the cluster under study, we used the position in CMD as the coordinate pair given by its colour and magnitude in the same units as PARSEC points, or

$$P_i = [c_i, m_i]. \quad (11)$$

With these coordinates in the CMD, we look for the region/polyhedron that $P_i \in R_j$. In case no region containing P_i is found, the star is considered non-interpolated. Next, in case of success in previous step, we look for which of the triangles associated with R_j contains P_i . This search will always return a positive result, since $P_i \in R_j$. The result of the previous step is the triangle $T^P = [\lambda_1, \lambda_2, \lambda_3]$ where $P_i \in T^P$ whose vertices have the properties age and mass, and we can perform the interpolation, once

$$P_i \in T^P \Rightarrow \gamma = f(\lambda_1, \lambda_2, \lambda_3). \quad (12)$$

Due to the nature of the theoretical PARSEC curves, the curves can define a surface that folds over itself, as can be seen in Figure 4. As a result, there will be stars contained in more than one triangle but belonging to different regions. In these cases, the researcher must provide another astrophysical criterion to choose the most appropriate solution.

RESULTS FROM EXPERIMENTAL PROCEDURES

Figure 5 presents the result for a single star belonging to cluster Collinder 205 (Cantat-Gaudin & Anders 2020). We present in Table 1 an extract of the results for the stars of this same cluster. A statistical view of the entire set of masses of these stars is shown in the histogram of Figure 6. Since we are dealing with optimization in an interpolation method, it is extremely important to estimate the execution times for different cases but for the same set of data. We chose the Collinder 205 cluster as the target of this analysis and made the same age and mass estimates of the stars following three different paths: a) estimation via distance calculation, b) triangulation for all points - without mapping via polygons, and c) the MatISG algorithm. This comparison is

presented in Table 2. Obviously, these time measurement values are dependent on the hardware and software used, and their interpretation must be in comparative terms.

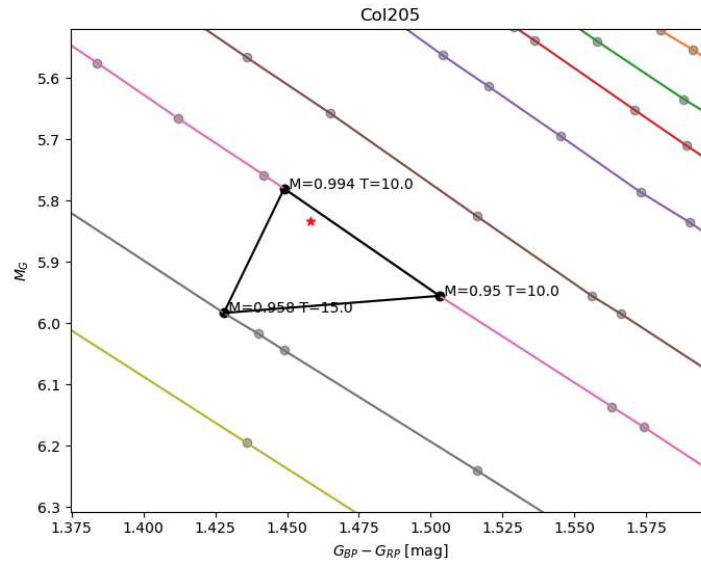


Figure 5. Result for the interpolation of a star (in red) with $w_{itnc} = 1.4583$ mag and $m = 5.8325$ mag from the Collinder 205 open cluster. The vertices of the triangle (in grey) are presented with their age and mass properties (M and T). The result for this star is age= 10.34×10^6 years and mass= 0.982 solar masses.

Table 1. Some results for mass and age obtained for the stars of the Collinder 205 cluster. The columns with indices "sup" and "inf" represent the error estimates for the magnitudes, which were calculated using the minimum polygon of each star in the *MatISG* algorithm. The first column is an identification of the star

i	$\log(\text{age})$ [year]	$\log(\text{age}_{sup})$ [year]	$\log(\text{age}_{inf})$ [year]	mass [solar masses]	mass _{sup} [solar masses]	mass _{inf} [solar masses]
681	6,522317697	0,021752303	0,045197697	0,749323931	0,000676069	0,049323931
240	6,704654896	0,170405104	0,005684896	0,749140534	0,000859466	0,049140534
585	7,602859704	0,096110296	0,301829704	1,147741542	0,001258458	0,008741542
553	6,883552052	0,116447948	0,008492052	1,09725381	0,00174619	0,00325381
145	6,675429071	0,023540929	0,073369071	0,748024808	0,001975192	0,048024808
389	7,168619955	0,007470045	0,168619955	0,747938932	0,002061068	0,000938932
1011	6,968770997	0,031229003	0,093710997	0,747914475	0,002085525	0,047914475
1009	7,117020278	0,059069722	0,117020278	0,947854265	0,002145735	0,003854265

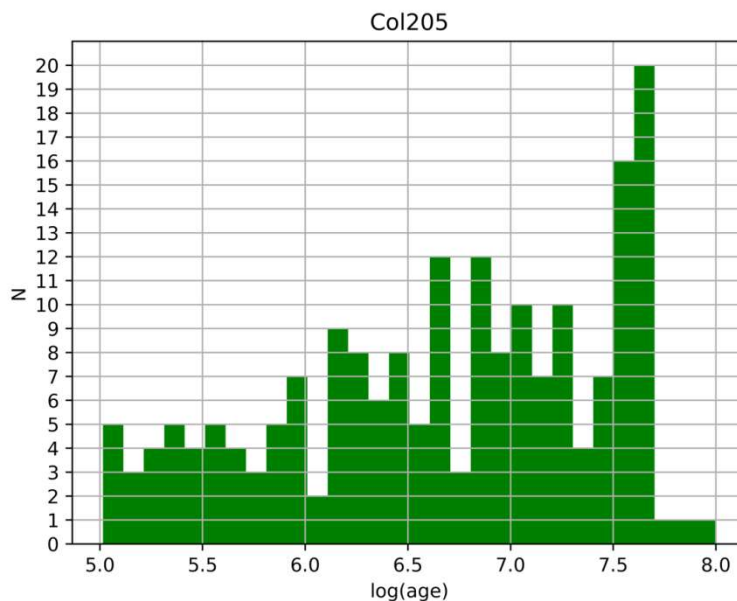


Figure 6. Histogram with the mass distribution obtained for the cluster Collinder 205

Table 2. Estimates of running time of algorithms in cases direct distance calculation, triangulation for all points without mapping via polygons, and the MaTISG algorithm

algorithm	time (s)
a distance direct	114.52
b only triangulation	3.31
c MaTISG	0.98

DISCUSSION AND CONCLUSION

We concluded that using a divide and conquer technique chosen for optimization of the problem in specific and general terms, the "golden rule", allows us to achieve good results in a much shorter time. In particular, the presented algorithm proved to be more than 100 times faster than the traditional path (calculation of distances to all points). Critical details of this algorithm, such as polygon calculation, triangulation, and interpolation, are available in libraries of many programming languages. This makes it possible to implement it without major difficulties in a wide spectrum of applications. For problems that require interpolations in a large set of sparse points in a high number of dimensions, the *MaTISG* algorithm presents itself as a good alternative, being economical and efficient.

REFERENCES

- Bressan A., Marigo P., Girardi L., Salasnich B., Dal Cero C., Rubele S., Nanni A., 2012, MNRAS, 427, 127
- Cantat-Gaudin, T. & Anders, F., 2020, Astronomy and Astrophysics, 2020A&A...633A..99C
- Delaunay, B. (1934). "Sur la sphère vide". Bulletin de l'Académie des Sciences de l'URSS, Classe des Sciences Mathématiques et Naturelles. 6: 793–800.
- Gaia Collaboration et al., 2017, A&A, 601, A19
- Goodin, W.R., McRae, G.J., Seinfeld, J.H., 1979, "A Comparison of Interpolation Methods for Sparse Data: Application do Wind and Concentration Fields", Journal of Applied Meteorology, v. 18, pp 761-771.
- Hertzprung, Ejnar (1908). "Über die Sterne der Unterabteilung c und ac nach der Spektralklassifikation von Antonia C. Maury". Astronomische Nachrichten. 179 (24): 373–380. Bibcode:1909AN....179..373H. doi:10.1002/asna.19081792402
- Hetem A., Gregorio-Hetem J., 2007, MNRAS, 382, 1707
- Hetem, A., & Gregorio-Hetem, J., 2019, MNRAS, 490, 2521-2541, doi:10.1093/mnras/stz2698
- Weisstein, E.W., "Jacobian". mathworld.wolfram.com. Archived from the original on 3 November 2017. Retrieved 2 May 2018.
